Interface Oral Health Science 2007: 95–104

Toughening of bioabsorbable polymer blend by microstructural modification

Mitsugu Todo[1]* **and Tetsuo Takayama**[2]*
[1]*Research Institute for Applied Mechanics;* [2]*Interdisciprinary Graduate School of Engineering Science, Kyushu University, Fukuoka 816-8580; Japan*
*todo@riam.kyushu-u.ac.jp, takayama@riam.kyushu-u.ac.jp

Abstract. In order to improve the phase morphology of bioabsorbable polymer blend of poly(lactic acid) (PLA) and poly (ε-caprolacton) (PCL), an additive with the isocyanate group, lysine tri-isocyanate (LTI), was used, and the effects of LTI addition on the fracture energy, J_{in}, and the related fracture micromechanism were investigated. The study showed that J_{in} effectively increases with an increase in LTI. Microscopic examination of the mode I fracture surfaces also exhibited that the size of the PCL phases dramatically decreases due to LTI addition, leading to the reduction of void formation and suppression of local stress concentration, and therefore resulting in the increase of the fracture energy. The improved miscibility also contributes to the ductility enhancement, which further increases the fracture energy. In order to improve the mechanical properties, such as the bending modulus and strength, the annealing process was conducted for PLA/PCL and PLA/PCL/LTI blends. The mechanical properties of both the blends effectively increased due to the strengthened structures by crystallization of PLA. J_{in} of PLA/PCL largely reduced by annealing; on the other hand, that of PLA/PCL/LTI effectively improved. The well-entangled structure of PLA/PCL/LTI results in the elongated ductile fracture of firmly connected fibrils; as a result, the energy dissipation during fracture initiation is largely increased.

Key words. poly(lactic acid), poly(ε-caprolacton), fracture energy, additive, crystallization

1 Introduction

Poly (lactic acid) (PLA) is one of the typical bioabsorbable polymers, which has been used as a biomaterial in medical fields such as orthopedics and oral surgery [1, 2]. PLA is, for example, utilized as bone fixation implants owing to its relatively high strength and stiffness. Its importance has led to many studies on its mechanical properties and fracture behavior [3–7] which found that the mode I fracture behavior of PLA is relatively brittle in nature. Therefore, blending with a ductile bioabsorbable polymer such as poly (ε-caprolacton) (PCL) has been adopted to improve the fracture energy of brittle PLA [8–13]. It was, however, also found that the immiscibility of PLA and PCL causes phase separation, and tends to lower the fracture energy especially when PCL content increases. It has recently been found

that addition of lysine tri-isocyanate (LTI) to PLA/PCL blend effectively improves their immiscibility [14–18], and therefore the fracture energy [13–18].

Although PCL blending effectively improves the brittleness of PLA and furthermore LTI addition results in dramatic improvement of the fracture energy of PLA/PCL, the fundamental mechanical properties, such as the bending strength and modulus of PLA/PCL and PLA/PCL/LTI, tend to be lower than the base polymer PLA as a result of the blending of ductile soft polymer PCL. It is known that these mechanical properties of PLA can be improved by crystallization using the annealing method [19]. However, the effects of crystallization on the mechanical properties of PLA/PCL and PLA/PCL/LTI blends have not yet been fully understood.

In this article, the effects of LTI addition and its content on a mode I fracture property, the fracture energy at initiation J_{in}, are presented. Fracture micro-mechanisms are also discussed on the basis of the microscopic results obtained using a polarizing-light optical microscope (POM) and a field emission scanning electron microscope (FE-SEM). The effects of annealing on the mechanical properties, such as the bending strength and modulus of PLA/PCL and PLA/PCL/LTI, were examined in the present study. J_{in} values of the annealed PLA/PCL and PLA/PCL/LTI were also evaluated, and compared to that of the quenched blends to assess the effectiveness of crystallization. Fracture micro-mechanism was also characterized by observing fracture surfaces using the FE-SEM. The fracture mechanism was then correlated with the macroscopic fracture energy.

2 Experimental

2.1 Materials and specimens

PLA/PCL and PLA/PCL/LTI blends were fabricated using PLA pellets (Lacty #9030, Shimadzu Kyoto, Japan) and PCL pellets (CelgreenH7, Daicel Chemistry Industries, Osaka, Japan), and LTI (Kyowa Hakko Chemical, Tokyo, Japan) by melt-mixing in a conventional melt-mixer at 180°C for 20 min and at a rotor speed of 50 rpm. The mixing ratio of PLA and PCL was fixed at 85:15 in weight fraction. For PLA/PCL/LTI, LTI contents were chosen to be 0.5, 1, 1.5, and 2 phr. The blend mixtures were then press-processed using a conventional hot press at 180°C and 30 MPa. Single-edge-notch-bend (SENB) specimens of $70 \times 10 \times 2\ mm^3$ with 5 mm notch were prepared from these plates for mode I fracture testing.

Some of the fabricated plates of PLA/PCL and PLA/PCL/LTI were annealed at 100°C for 3 h using a forced convection oven and then naturally cooled down to room temperature. For the annealed PLA/PCL/LTI, LTI content was fixed at 1 phr. Bean specimens of $70 \times 10 \times 2\ mm^3$ were prepared from the annealed plates to evaluate bending mechanical properties such as the modulus and strength. SENB specimens were also processed from the annealed plates to measure the mode I fracture energy.

The microstructures of the prepared specimens were characterized by observing the fracture surfaces of cryo-fractured SENB specimens prepared under liquid nitrogen environment using FE-SEM.

2.2 Crystallinity and molecular weight measurement

The enthalpy of crystallization and melting, dH_c and dH_m, of the quenched and the annealed PLA/PCL and PLA/PCL/LTI were determined by a differential scanning calorimeter (DSC). Small pieces of the blends were heated under nitrogen gas flow at a rate of 10°C/min for DSC measurements. The crystallinity of PLA, $x_{c,PLA}$, in the blends having constant PLA content, X_{PLA}, was evaluated according to the following formula [19]:

$$x_{c,PLA}(\%) = \frac{100 \times (dH_m + dH_c)}{93 \times X_{PLA}} \tag{1}$$

where 93 (J/g of the polymer) is the enthalpy of melting of the PLA crystal having the infinite crystal thickness reported by Fischer et al. [20].

The weight-average molecular weight, M_w, of the prepared samples was evaluated in chloroform at 40°C by a GPC system with a spherical porous gel made of a styrene–divinylbenzene copolymer using polystyrene standards.

2.3 Mode I fracture and bending tests

Three-point-bend-type fracture tests of the SENB specimens were conducted using a servo-hydraulic testing machine at a loading rate of 1 mm/min. Time histories of load and displacement data were recorded using a digital recorder, and later, load–displacement relationship was evaluated from these data. The critical *J*-integral value, J_{in}, at crack initiation was obtained as the fracture energy using the following formula:

$$J_{in} = \frac{\eta U_{in}}{B(W-a)} \tag{2}$$

where U_{in} is the critical energy, B the specimen thickness, W the specimen width, a the initial crack length, and η the geometrical correction factor, which is equal to 2 for the standard SENB specimen. The critical point corresponding to crack initiation was defined as the point at which the specimen rigidity dropped suddenly due to the onset of crack propagation [15].

Three-point bending tests of the beam specimens were performed at a loading-rate of 10 mm/min using the servo-hydraulic testing machine, and the load–displacement curves were obtained as described above. Bending modulus, E, and bending strength, σ_f, were then evaluated from the linear portion of the load–displacement curves and the maximum load, respectively, using the following formulae:

$$E = \frac{L^3}{4bh^3} S \quad \text{and} \quad \sigma_f = \frac{3PL}{2bh^2} \tag{3}$$

where S is the initial slope of the load–displacement curve. L, b, and h are the span, the width, and the thickness, respectively, and P is the maximum load.

2.4 Microscopic observation

For each of PLA, PLA/PCL and PLA/PCL/LTI specimens, a thin section was prepared using the petro-graphic thin-sectioning technique from the region in the vicinity of the crack-tip where process zone was developed in the mode I fracture test. The thin-sectioned samples were then observed using POM to characterize the mechanism of process zone formation. Fracture surfaces of the mode I fracture specimens were also observed using FE-SEM to characterize the fracture mechanism and the effect of LTI addition and annealing on the fracture behavior.

3 Results and discussion

3.1 Effect of LTI addition on the fracture energy of PLA/PCL

3.1.1 Phase morphology

FE-SEM micrographs of cryo-fractured surfaces of PLA/PCL and PLA/PCL/LTI are shown in Fig. 1. Spherical features appeared on the micrograph are thought to

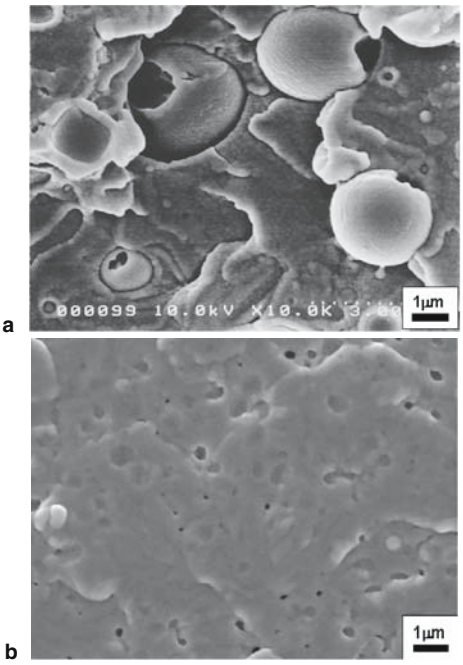

Fig. 1. FE-SEM micrographs of cryo-fracture surfaces of PLA/PCL and PLA/PCL/LTI **a** PLA/PCL; **b** PLA/PCL/LTI

be PCL-rich phases [9]. These micrographs clearly showed that the size of the PCL-rich phase dramatically decreases by LTI addition. It is thus presumed that LTI addition effectively improves the miscibility of PLA and PCL. This is thought to be related to the following chemical reaction, that is, the hydroxyl group of PLA and the isocyanate group of LTI creates a urethane bond:

$$HO–R' + R–N=C=O \rightarrow R–NHCOO–R'$$

3.1.2 Fracture energy and mechanisms

Dependence of Jin on LTI content is shown in Fig. 2. It is seen that J_{in} of PLA/PCL is a little larger than that of PLA, indicating the effectiveness of PCL blend on J_{in} is very low. J_{in} of PLA/PCL is effectively improved by LTI addition, and J_{in} increases with increase in LTI content up to 1.5 phr. There is no difference of J_{in} between 2 and 1 phr of LTI addition, suggesting that the improvement of J_{in} is saturated with about 1.5 phr of LTI.

POM micrographs of crack growth behaviors in PLA, PLA/PCL, and PLA/PCL/LTI are shown in Fig. 3. Craze-like features are clearly seen in front of the crack-tip of the pure PLA in Fig. 3a. This kind of crack-tip damage is broadened by PCL blending as shown in Fig. 3b. With LTI addition, the craze-like feature is no longer generated, and instead, the crack-tip region is plastically deformed, very similar to the crack-tip deformation in ductile plastics and metal. It is known that this kind of plastic deformation dissipates more energy than the craze-like damage, resulting in the greater fracture energy. It is therefore thought that LTI addition to PLA/PCL dramatically changes the crack-tip deformation mechanism; as a result, J_{in} is greatly improved.

FE-SEM micrographs of fracture surfaces in the vicinity of the initial notch-tip are shown in Fig. 4. The fracture surface of PLA is very smooth, corresponding

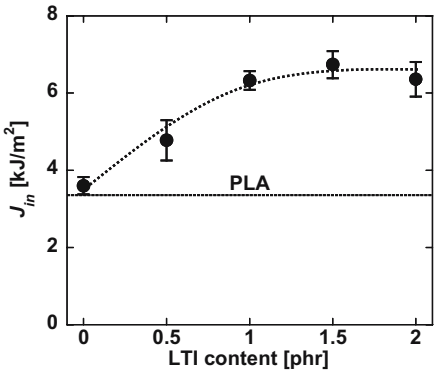

Fig. 2. Dependence of the fracture energy, J_{in}, on LTI content

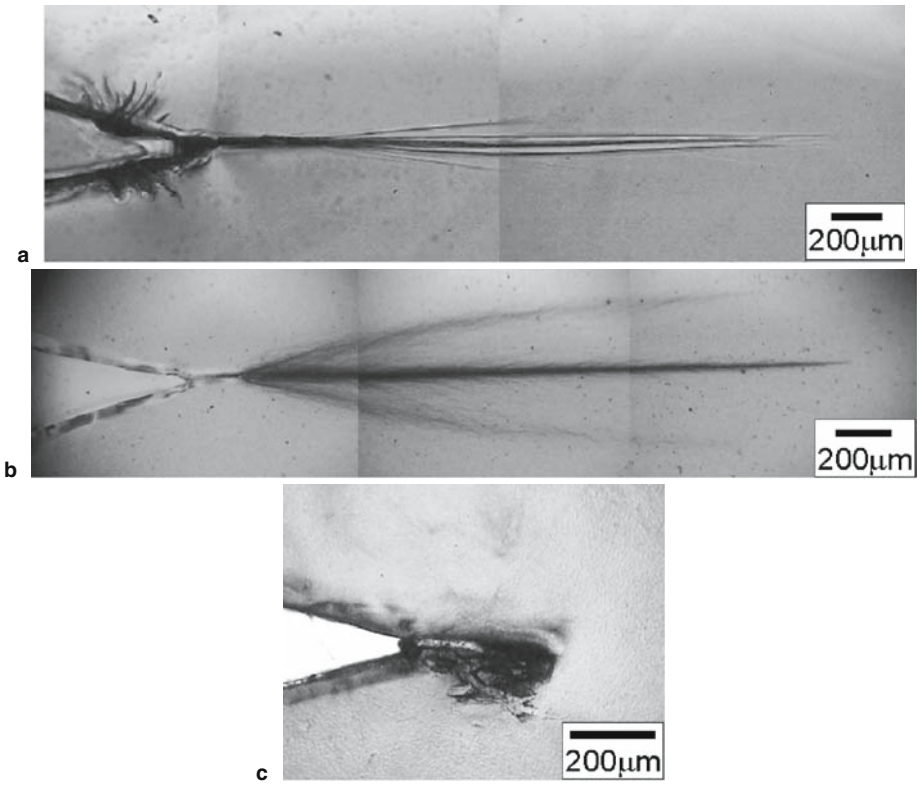

Fig. 3. POM micrographs of crack growth behaviors. **a** PLA; **b** PLA/PCL; **c** PLA/PCL/LTI

to a brittle fracture behavior with low fracture energy. The surface roughness increases with the existence of elongated PCL and cavities by PCL blending. These cavities are thought to be created by debonding of the PCL-rich phases from the surrounding PLA matrix phase and usually cause local stress concentration in the surrounding regions. Thus, this kind of cavitation tends to lower the fracture energy because of the local stress concentration, and compensates to the increase in fracture energy due to the ductile deformation of PCL. This is the reason for the slight improvement of J_{in} in PLA/PCL shown in Fig. 2. It is clearly seen from Fig. 4c that cavities do not exist on the fracture surface of PLA/PCL/LTI, indicating that the miscibility of PLA and PCL improves due to LTI addition. In addition, elongated structures are more on PLA/PCL/LTI than PLA/PCL. Thus, extensive ductile deformation associated with disappearance of cavitation is the primary mechanism of the dramatic improvement of J_{in}.

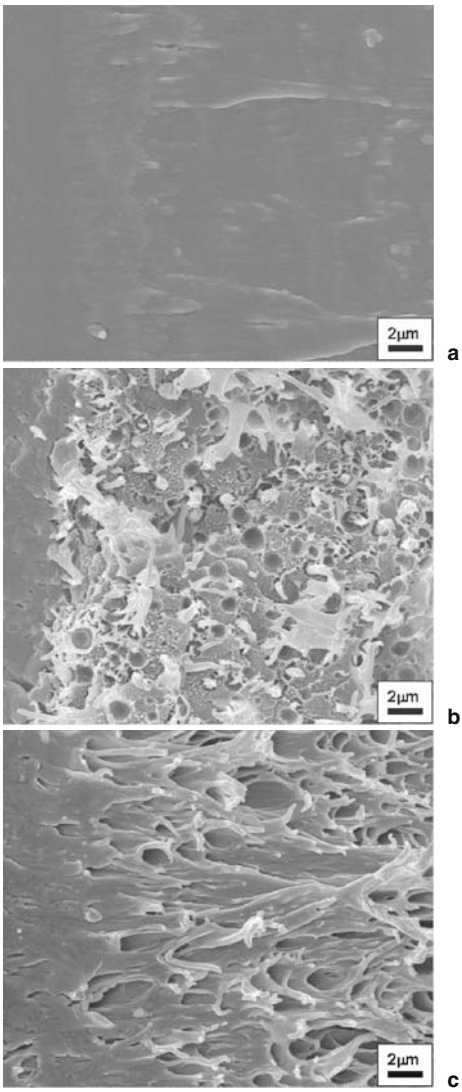

Fig. 4. FE-SEM micrographs of mode I fracture surfaces. **a** PLA; **b** PLA/PCL; **c** PLA/PCL/LTI

3.2 Effect of annealing on the mechanical properties and fracture energy of PLA/PCL and PLA/PCL/LTI

3.2.1 Microstructure and microstructural properties

FE-SEM micrographs of the cryo-fracture surfaces of the annealed PLA/PCL and PLA/PCL/LTI are shown in Fig. 5. By comparing Fig. 5 with Fig. 1, the effect of annealing on the micro-structural change is recognized as a cauliflower-like surface, indicating the formation of PLA spherulites. Crystallinity, $x_{c,PLA}$, and molecular

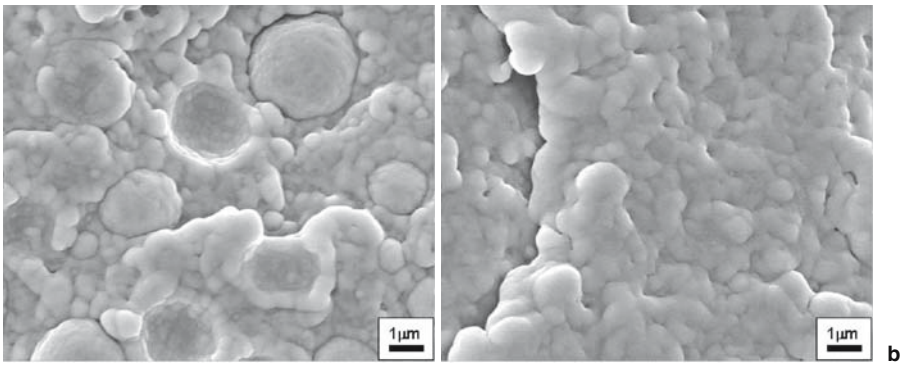

Fig. 5. FE-SEM micrographs of cryo-fracture surfaces of annealed blends. **a** PLA/PCL; **b** PLA/PCL/LTI

Table 1. Effect of annealing on $x_{c,\,PLA}$ and M_w of PLA/PCL and PLA/PCL/LTI

Polymer blend	Process condition	$x_{c,PLA}$ (%)	M_w (g/mol)
PLA/PCL	Quenching	11.4	1.03×10^5
	Annealing	45.6	9.08×10^4
PLA/PCL/LTI	Quenching	4.8	1.13×10^5
	Annealing	36.6	1.52×10^5

Table 2. Effect of annealing on the bending and fracture properties of PLA/PCL and PLA/PCL/LTI

Material	Process condition	E (GPa)	σ_f (MPa)	J_{in} (kJ/m^2)
PLA		3.70	103.2	3.32
PLA/PCL	Quenching	3.26	93.5	3.60
	Annealing	3.74	95.7	0.61
PLA/PCL/LTI	Quenching	3.06	85.6	6.33
	Annealing	3.56	100.3	8.68

weight, M_w, are shown in Table 1. It is clearly seen that $x_{c,PLA}$ increases dramatically with annealing. M_w of PLA/PCL slightly decreases by annealing and this might be due to thermal degradation of molecules during annealing at 100°C for 3 h. On the other hand, M_w of PLA/PCL/LTI increases by annealing. This is thought to be attributable to the polymerization by urethane bond formation.

3.2.2 Bending and fracture properties

Effect of annealing on the bending mechanical properties, E and σ_f, of PLA/PCL and PLA/PCL/LTI are shown in Table 2. These values of the pure PLA are also

shown in the table. For both the polymer blends, E and σ_f tend to increase by annealing. Annealing causes crystallization of PLA, as indicated by increase in $x_{c,PLA}$ (see Table 1), and therefore, likely to strengthen the structure of PLA and the blends, resulting in the increase of E and σ_f. It should be noted that E values of both the blends and σ_f of PLA/PCL/LTI become very close to those of PLA.

Effects of annealing on J_{in} are also shown in Table 1. J_{in} of PLA/PCL largely degrades by annealing; on the other hand, J_{in} of PLA/PCL/LTI effectively improves by 161% due to annealing.

3.2.3 Fracture mechanism

Field emission scanning electron microscope micrographs of mode I fracture surfaces of the annealed blends are shown in Fig. 6. For the annealed PLA/PCL, ruptured PLA fibrils are created on the fracture surface; on the other hand, elongated structures of the spherical PCL phases are observed in the quenched PLA/PCL as shown in Fig. 4b. As reported by Park et al. previously that annealing process tends to reduce the fracture energy of PLA [5–7] due to the embrittlement of the PLA structure by crystallization, for PLA/PCL, the PLA-rich phases are likely to become brittle by annealing and because of the phase separation caused by the immiscibility of PLA and PCL, J_{in} degrades. For the annealed PLA/PCL/LTI, elongated entangled fibril structures generated by the chemical bonding between PLA and PCL molecules through LTI addition are observed as also seen in the quenched PLA/PCL/LTI (Fig. 4c), and these fibrils are firmly connected to each other due to the crystallization of PLA. This kind of micro-structural change is thought to result in the improvement of J_{in}.

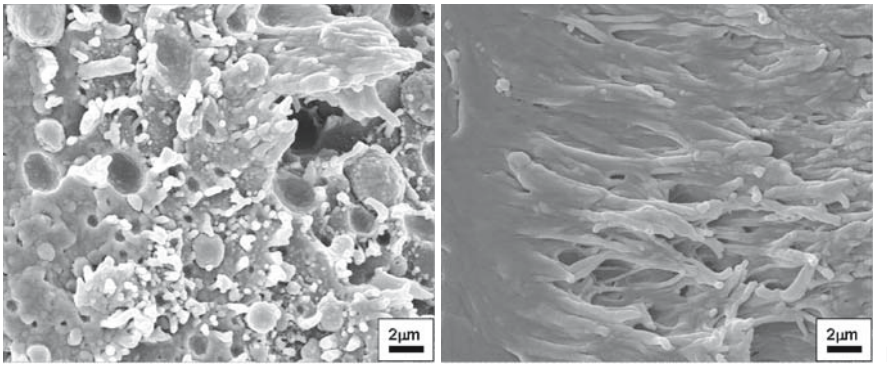

Fig. 6. FE-SEM micrographs of mode I fracture surfaces of annealed blends. **a** PLA/PCL; **b** PLA/PCL/LTI

4 Summary

Effects of LTI additive on the fracture energy, J_{in}, and the fracture micro-mechanism of PLA/PCL polymer blend were investigated, and furthermore, effects of annealing process on the bending mechanical properties, E and σ_f, and J_{in} of PLA/PCL and PLA/PCL/LTI blends were assessed and the micro-structural modification due to annealing was characterized. The results obtained are summarized as follows:

(1) The miscibility of PLA and PCL is effectively improved by LTI addition; as a result, the phase morphology of PLA/PCL is dramatically changed such that the size of the PCL-rich phases become small.
(2) J_{in} of PLA/PCL is effectively improved by LTI addition, and increases with increase in LTI up to 1 phr. The improvement is saturated more than 1 phr of LTI.
(3) E of both the polymer blends and σ_f of PLA/PCL/LTI are effectively improved by annealing. Especially, E of the blends becomes very close to that of the pure PLA. These improvements of the mechanical properties are thought to be related to the strengthened structures of the blends due to the crystallization of PLA phase by annealing.
(4) J_{in} of PLA/PCL largely degrades by annealing as a result of embrittlement of the PLA phases. On the contrary, J_{in} of PLA/PCL/LTI is effectively improved by annealing. The well-entangled structure of PLA/PCL/LTI results in the elongated ductile fracture of firmly connected fibrils; as a result, the energy dissipation during fracture initiation is largely increased.

References

1. Mohanty AK, Misra M, Hinrichsen G (2000) Macromol Mater Eng 276/277:1–24
2. Higashi S, Tamamoto T, Nakamura T, et al (1986) Biomaterials 7:183–187
3. Todo M, Shinohara N, Arakawa K (2002) J Mater Sci Lett 21:1203–1206
4. Todo M, Shinohara N, Arakawa K, et al (2003) Kobunshi Ronbunshu 60:644–651
5. Park SD, Todo M, Arakawa K (2004) J Mater Sci 39:1113–1116
6. Park SD, Todo M, Arakawa K (2004) Key Eng Mater 261/263:105–110
7. Park SD, Todo M, Arakawa K (2005) J Mater Sci 40:1055–1058
8. Tsuji H, Ikada Y (1996) J Appl Polym Sci 60:2367–2375
9. Todo M, Park SD, Takayama T, Arakawa K (2007) Eng Frac Mech 74:1872–1883
10. Wang L, Ma W, Gross RA, et al (1998) Polym Degrad Stab 59:161–168
11. Hiljanen M, Varpomaa P, Sppala J, et al (1996) Macromol Chem Phys 197:1503–1523
12. Meredith JC, Amis EJ (2000) Macromol Chem Phys 201:733–739
13. Tsuji H, Yamada T, Suzuki M, et al (2003) Polym Int 52:269–275
14. Dell' Erba R, Groeninckx G, Maglio G, et al (2001) Polymer 42:7831–7840
15. Harada M, Hayashi H, Iida K, et al (2003) Polym Prepr 52:965
16. Takayama T, Todo M, Arakawa K, et al (2006) Trans Jpn Soc Mech Eng 72:713–718
17. Takayama T, Todo M (2006) J Mater Sci 41:4989–4992
18. Takayama T, Todo M, Tsuji H, et al (2006) J Mater Sci 41:6501–6504
19. Tsuji H, Ikada Y (1995) Polymer 36:2709–2716
20. Fischer EW, Sterzel HJ, Wegner G (1973) Kolloid-Z u Z Polym 251:980